

# Transmission Properties of Defect Modes with Different Defect Layer Geometries in One-Dimensional Photonic Crystals

Ali Çetin

Department of Physics, Faculty of Science and Letters, Eskisehir Osmangazi University,  
Meşelik Campus, Eskişehir-Turkey

---

**ABSTRACT:** In this paper, the transmittance of transverse electric field (TE) in one-dimensional photonic crystals (1D PC's) with different defect layer geometries is theoretically investigated in visible region by using finite-difference time-domain (FDTD) method.  $TiO_2$  is used as higher refractive index material,  $SiO_2$  is used as lower refractive index material and  $Al_2O_3$  is used as defect layer material. Our results show that defect layer geometry effect TE transmittance peak value and position therefore we achieved the optimum geometry for the highest transmittance. We also find that if we take the defect layer material  $Al_2O_3$ , thickness 80 nm and position as  $(AB)_4C(AB)_4$ , highest transmittance peak value occurred.

**KEYWORDS** - Photonic crystal, Defect Layer Geometry, Visible Region, FDTD Method.

---

Date of Submission: 10-09-2020

Date of Acceptance: 25-09-2020

---

## I. INTRODUCTION

Photonic crystals (PCs) are optical nanostructures which dielectric constants change periodically [1]. Because of this periodic change PCs structures have forbidden frequency range called as the photonic band gap (PBG) that electromagnetic waves not propagate in this region [2]. This property of PCs provides us to control the propagate of light [3]. PCs can be periodic in one-dimensional (1D), two-dimensional (2D) and three-dimensional (3D) [4]. 1D PCs attract attention because of easily investigated and fabricated. In 1D PCs, dielectric constants are periodic in one-dimension and used as low-loss optical waveguides, high-efficiency semiconductor lasers, dielectric reflecting mirrors, light-emitting diodes, optical switches, high-Q resonators, antennas, optical filters, frequency selective surfaces, antireflection coatings etc [5-7].

In PCs, produced defects break the periodicity and leads to the appearance of localized modes in the forbidden bands which named defect modes [8, 9]. Properties of defect layer parameters such as defect layer geometry, material, thickness and position affect the behavior of defect modes.

In recent years, too many theoretically and experimentally investigations carried out effects on transverse electric (TE) and magnetic (TM) field's transmittance and reflectance of defects in PCs [10, 11]. In these investigations, defect layer geometries are considered to be linear.

In this paper, we have examined the effects of the different defect layer geometries on TE transmittance. The highest TE transmittance geometry has obtained in visible range for 1D PCs. Also material, thickness and position of defect layer have optimized for the highest transmittance.

To investigate PCs different theoretical techniques can be used such as transfer matrix method (TMM) [12], the plane wave method (PWM) [13] and finite-difference time-domain method (FDTD) [14, 15]. We prefer FDTD method for theoretical analysis because of its simplicity, applicability and losses of propagation fields are smaller from other approximation methods. We used OptiFDTD software [16] for our transmittance spectra simulations which based on the finite-difference time-domain method (FDTD) method.

## II. THEORETICAL METHOD

FDTD method solves the Maxwell equations in complex geometries. This method solves the transverse electric (TE) and magnetic fields (TM) by depending on space and time. In FDTD method, space and time axis are divided in regular grids along the axis direction as known Yee cells. A certain time step is determined for iterations. After the iterations TE and TM fields can be calculated in 1D PCs.

Maxwell equation for isotropic linear medium is

$$\nabla \times \mathbf{H} = \varepsilon \frac{\partial \mathbf{E}}{\partial t} + \sigma \mathbf{E} \quad (1)$$

Where  $\mathbf{E}$  is the electric field,  $\mathbf{H}$  is the magnetic field,  $\varepsilon$  is the dielectric permittivity and  $\sigma$  is the electric loss of the medium. If we suppose electromagnetic wave propagate along z direction in 1D PC, Eq. 1 can be written as,

$$-\frac{\partial H_y}{\partial z} = \epsilon \frac{\partial E_x}{\partial t} + \sigma E_x \quad (2)$$

In 1D Yee cells, if we suppose integer k as number of space step  $\Delta z$  and integer n as time steps  $\Delta t$  along the z direction then Eq. 2 is expressed as,

$$E_x^{n+1}(k) = \frac{1 - \frac{\sigma(m)\Delta t}{2\epsilon(m)}}{1 + \frac{\sigma(m)\Delta t}{2\epsilon(m)}} \times E_x^n(k) - \frac{\frac{\Delta t}{\epsilon(m)}}{1 + \frac{\sigma(m)\Delta t}{2\epsilon(m)}} \times \frac{H_y^{n+1/2}(k+\frac{1}{2}) - H_y^{n+1/2}(k-\frac{1}{2})}{\Delta z} \quad (3)$$

Eq. 3 provides us to calculate TE values for each space and time steps.

Frequency domain transmission spectrum can be obtained by the Fourier transform of the time domain data. The band structures of defective 1D PC can have a wide variety in electromagnetic properties. For determination of boundary conditions perfectly matched layers (PMLs) and periodic boundary conditions (PBC) can be use [17, 18].

### III. RESULTS AND DISCUSSION

We consider PCs which forms are  $(AB)_4C(AB)_4$  shown layout of PCs in Fig 1. Wafer dimensions are  $10\mu\text{m} \times 10\mu\text{m}$  and the wafer material taken air. The layer A, B and C represent  $\text{SiO}_2$ ,  $\text{TiO}_2$  and  $\text{Al}_2\text{O}_3$  where refractive indexes of layers are  $n_a = 1.55$ ,  $n_b = 2.97$ ,  $n_c = 1.77$  at  $\lambda = 543.5 \text{ nm}$  [19] and the structure layer thicknesses are chosen  $d_a = 88 \text{ nm}$ ,  $d_b = 46 \text{ nm}$  and  $d_c = 80 \text{ nm}$  according to quarter wave stack condition ( $n \cdot d = \lambda/4$ ) respectively. Red vertical line represents the input plane which taken to Gauss modulated continuous wave. The input plane wavelength is 543.5 nm (He-Ne laser) [20] and propagate at z direction. The green point is observation points which observe transmission of TE.

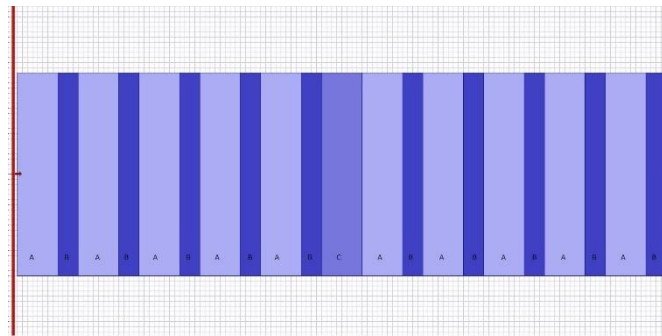
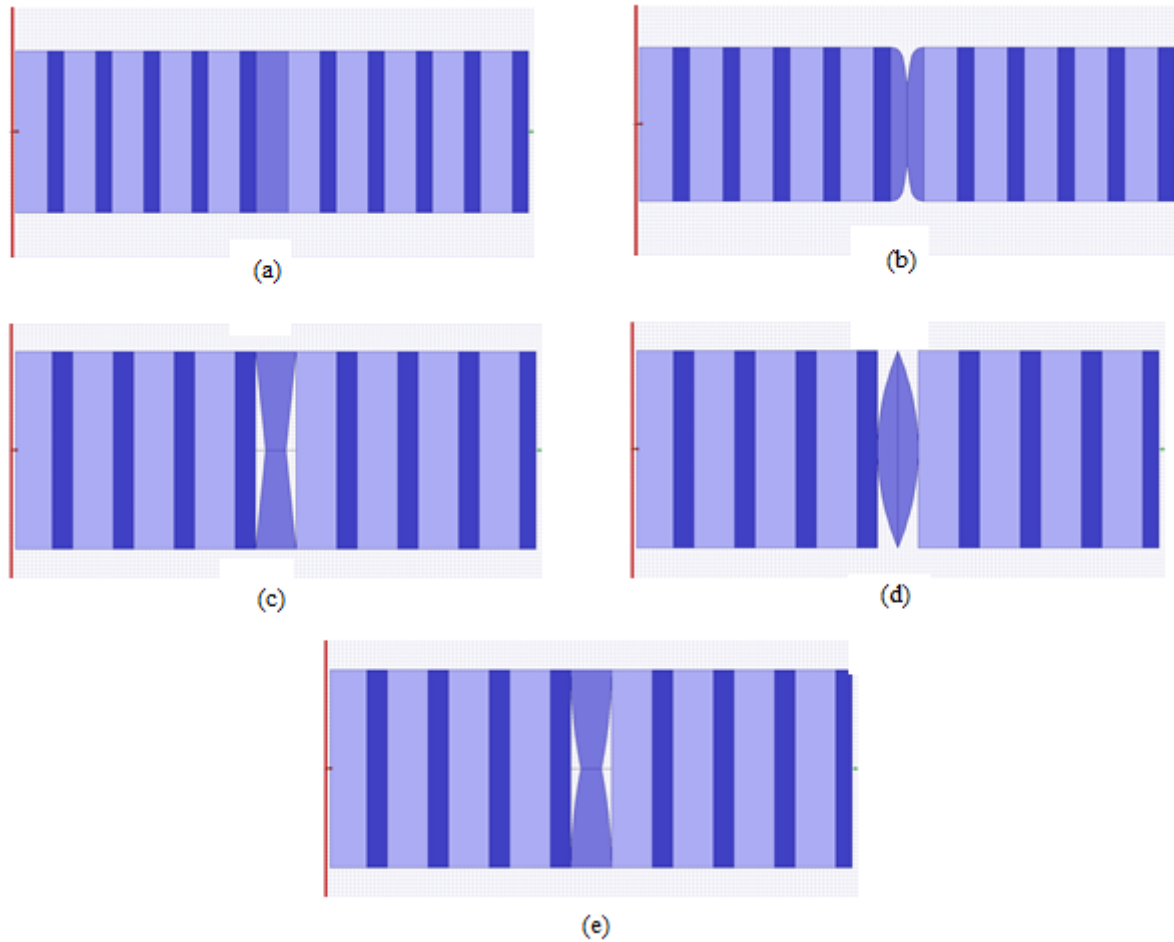


Fig. 1. Fig. 1 Layout of 1D PCs.

In order to investigate defect layer geometry on TE transmittance we consider different defect layer geometries as shown in Fig. 2. The TE transmittance spectra of these different PCs structures are shown in Fig. 3. The transmittance peaks were occurred in visible range for all structures. TE transmittance peak values and position for designed defect layer geometries are different. The minimum transmittance peak value occurred in Fig. 2 (c) at 602 nm rate for % 51 and maximum transmittance peak value occurred in Fig. 2 (e) at 513 nm rate for % 72. These results suggest us for our purposes PC shown in Fig. 2 (e) is more suitable to be the defect layer geometry for TE transmittance.

The defect layer material is an important performance factor for the TE transmittance. In Fig. 4 the transmittance spectra of 1D PCs with different defect layer materials such as  $\text{Al}_2\text{O}_3$ ,  $\text{LiNbO}_3$ ,  $\text{ZnO}$ ,  $\text{GaAs}$  and  $\text{Si}$  shown. The other parameters are same with Fig. 2 (e).

The minimum transmittance peak value occurred while the defect layer material is  $\text{Si}$  at 602 nm rate for % 40 and maximum transmittance peak value occurred while the defect layer material is  $\text{Al}_2\text{O}_3$  at 513 nm rate for % 72 as shown in Fig. 4. As the refractive index of the defect layer increases, the maximum transmittance peak value decreases. For  $\text{Si}$  and  $\text{GaAs}$  second peaks occurred at 435 nm and 432 nm respectively, also photonic band gap (PBG) occurred for  $\text{GaAs}$  between 506-533 nm. With the refractive index of defect layer increases, maximum transmittance peaks move higher wavelengths and second peaks occurred at lower wavelengths. From these results we can choose the  $\text{Al}_2\text{O}_3$  as appropriate material for our purposes.



**Fig. 2.** Layout of PCs with different defect layer geometries. (a) Common geometry, (b) Exponential taper geometry. (c) Linear taper geometry, (d) Hyperbolic lens geometry. (e) Parabolic taper geometry.

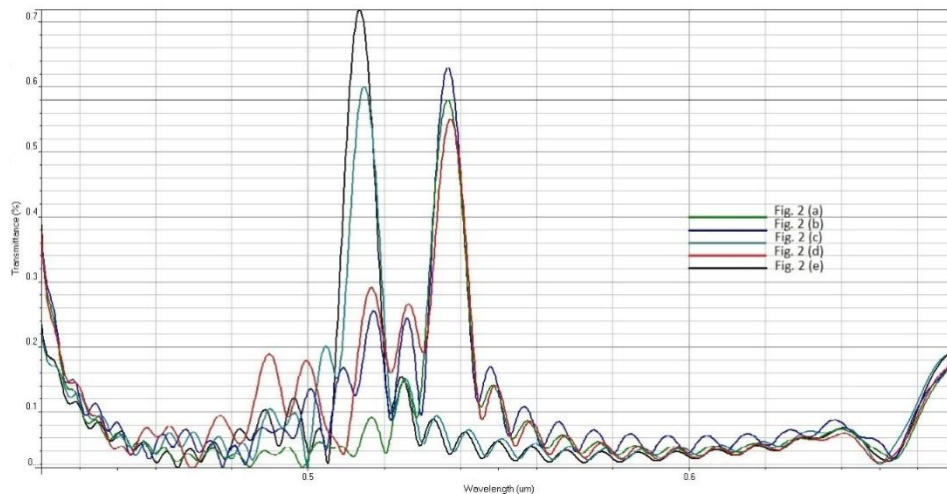


**Fig. 3.** TE transmittance spectra of PCs with different defect layer geometries.

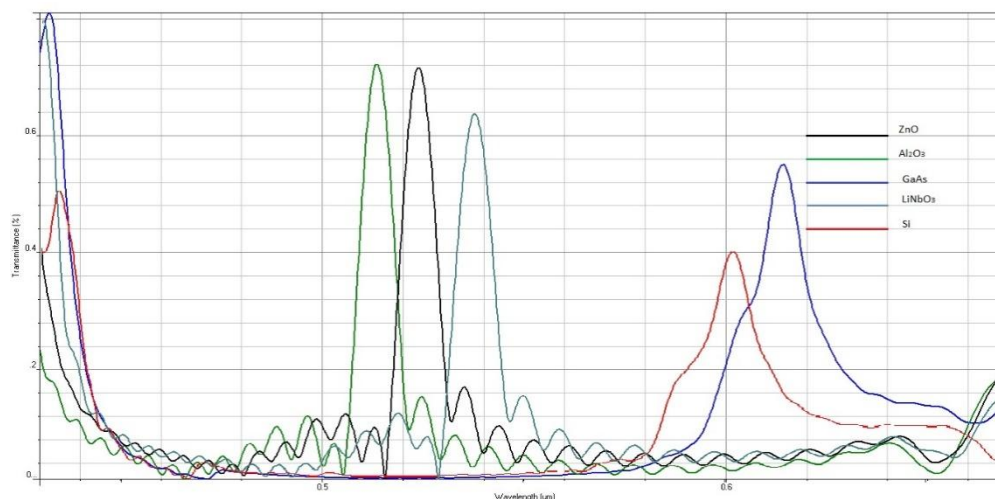


**Fig. 4.** TE transmittance of PCs with different defective layers.

For investigate the effect of defect layer thickness over TE transmittance we get defect layer thickness as 80 nm, 102 nm, 154 nm, 184 nm and 307 nm ( $n \cdot d = \lambda/4$ ,  $n \cdot d = \lambda/3$ ,  $n \cdot d = \lambda/2$ ,  $n \cdot d = 3\lambda/5$  and  $n \cdot d = \lambda$ ) shown in TE transmittance spectra of PCs with different defect layer thickness in Fig. 5. Here defect layer geometry is same as Fig. 2(e) and defect layer material is  $\text{Al}_2\text{O}_3$ .

From Fig. 5 the minimum transmittance peak value occurred while the defect layer thickness is 307 nm at 548 nm rate for % 14 and maximum transmittance peak value occurred while the defect layer thickness is 80 nm at 513 nm rate for % 72. The maximum transmittance peaks move to the higher wavelengths as increase the defect layer thickness. For 184 nm the maximum transmittance peak was disappeared in higher wavelengths and for 184 nm and 154 nm thicknesses second transmittance peaks occur from lower wavelengths. Thus the maximum transmittance peaks can be controlled by changing the thickness of defect layers.

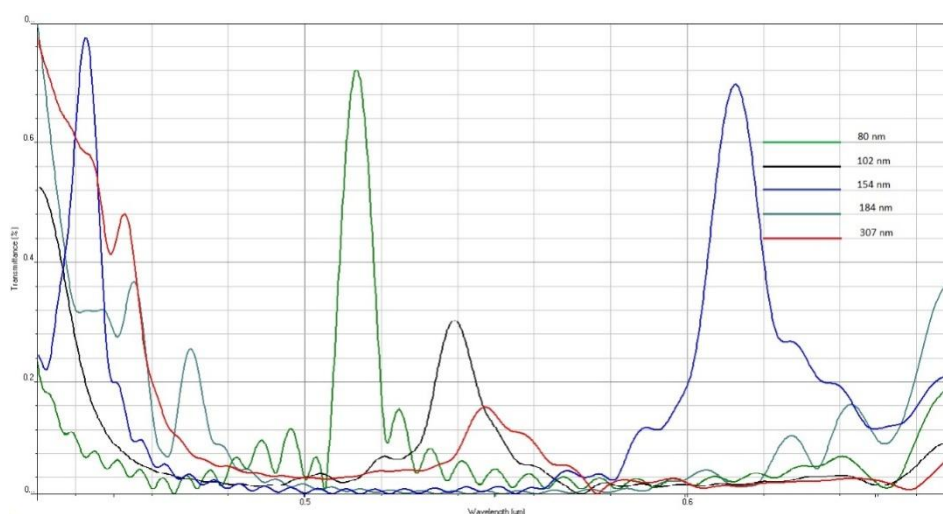


**Fig. 5.** TE transmittance of PCs with different defect layer thicknesses.

Finally, we examined effect of defect layer position on TE transmittance by studying  $(\text{AB})_2\text{C}(\text{AB})_6$ ,  $(\text{AB})_3\text{C}(\text{AB})_5$ ,  $(\text{AB})_4\text{C}(\text{AB})_4$ ,  $(\text{AB})_5\text{C}(\text{AB})_3$ ,  $(\text{AB})_6\text{C}(\text{AB})_2$  structures.

TE transmittance spectra of PCs with different defect layer positions are shown in Fig. 6. Defect layer geometry is same as Fig. 2(e), defect layer material is  $\text{Al}_2\text{O}_3$  and defect layer thickness is 80 nm. The minimum transmittance peak value occurred in  $(\text{AB})_2\text{C}(\text{AB})_6$  at 522 nm for % 15 and maximum transmittance peak value occurred in  $(\text{AB})_4\text{C}(\text{AB})_4$  at 513 nm for % 72. Also for  $(\text{AB})_6\text{C}(\text{AB})_2$  second transmittance peak occurred at lower wavelengths. Thus, the maximum peak values and positions can be controlled by changing the defect layer position.

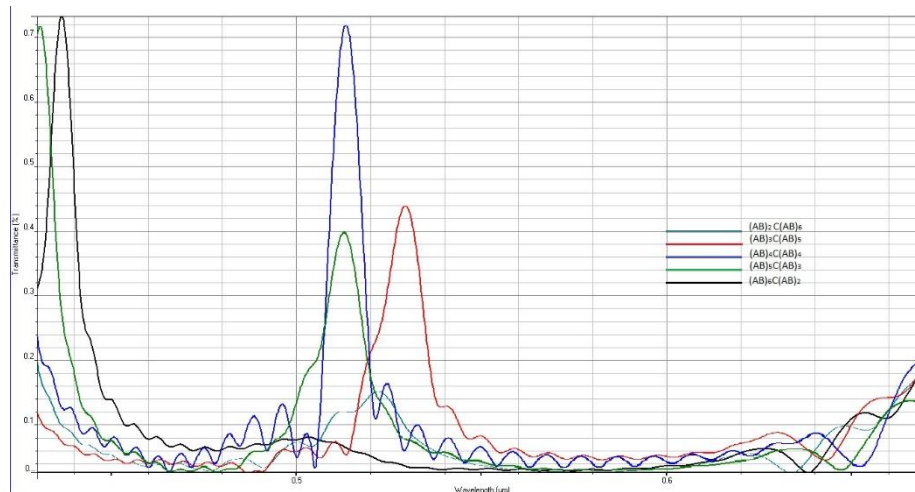


Fig. 6. TE transmittance of PCs with different defect layer positions.

#### IV. CONCLUSION

We have theoretically investigated the effect of defect layer geometries on TE transmittance in 1D PCs at visible range. Our simulations show that defect layer geometries affect the transmittance of TE. Different defect layer geometries studied and the defective layer geometry with maximum transmittance was determined. Also we analyzed defect layer material, thickness and position on TE transmittance. PC structure of  $\text{Al}_2\text{O}_3$  material at 80 nm thickness and at  $(\text{AB})_4\text{C}(\text{AB})_4$  position showed maximum TE transmittance. These results provide us designing and manufacturing new types of 1D PCs for optical applications at visible region.

#### ACKNOWLEDGEMENT

The author would like to thank the Optiwave System Inc. for free OptiFDTD 32 bit program.

#### REFERENCES

- [1]. S. Kuzuki, *Optical properties of photonic crystals*, (Springer Science & Business Media, 2004).
- [2]. P. St J, Photonic band gaps, *Physics world*, 5(8), 1992, 37-42.
- [3]. J. D. Joannopoulos, R. D. Meade, J. N. Winn, *Photonic crystals: molding the flow of light* (Princeton university press, 2011).
- [4]. Á. Notomi, Theory of light propagation in strongly modulated photonic crystals: Refractionlike behavior in the vicinity of the photonic band gap, *Physical Review B*, 62(16), 2000, 10696-10705.
- [5]. K. Busch, S. Lölkes, R. B. Wehrspohn and H. Föll, *Photonic crystals: advances in design, fabrication, and characterization*, (John Wiley & Sons, 2006).
- [6]. V. Berger, Photonic crystals and photonic structures, *Current Opinion in Solid State and Materials Science*, 4(2), 1999, 209-216.
- [7]. M. A. Kats, R. Blanchard, P. Genevet, and F. Capasso, Nanometre optical coatings based on strong interference effects in highly absorbing media. *Nature Materials*, 12(1), 2013, 20-24.
- [8]. Y. K. Ha, Y. C. Yang, Y. E. Kim, H. Y. Park, C. S. Kee, H. Lim and J. C. Lee, Tunable omnidirectional reflection bands and defect modes of a one-dimensional photonic band gap structure with liquid crystals, *Applied Physics Letters*, 79(1), 2001, 15-17.
- [9]. X. Xiao, W. Wenjun, L. Shuhong, Z. Wanquan, Z. Dong, D. Qianqian and Z. Bingyuan, Investigation of defect modes with  $\text{Al}_2\text{O}_3$  and  $\text{TiO}_2$  in one-dimensional photonic crystals. *Optik*, 127(1), 2016, 135-138.
- [10]. Y. Zongfu, Z. Wang and S. Fan, One-way total reflection with one-dimensional magneto-optical photonic crystals, *Applied Physics Letters*, 90(12), 2007, 121133.
- [11]. S. G. Tikhodeev, A. L. Yablonskii, E. A. Muljarov, N. A. Gippius and T. Ishihara, Quasiguidded modes and optical properties of photonic crystal slabs. *Physical Review B*, 66(4), 2002, 045102-1-045102-17.
- [12]. Z. Y. Li, L. L. Lin, Photonic band structures solved by a plane-wave-based transfer-matrix method, *Physical Review E*, 67(4), 2003, 046607.
- [13]. S. Shi, C. Chen and D. W. Prather, Revised plane wave method for dispersive material and its application to band structure calculations of photonic crystal slabs. *Applied Physics Letters*, 86(4), 2005, 043104.
- [14]. M. Qiu, Analysis of guided modes in photonic crystal fibers using the finite-difference time-domain method, *Microwave and Optical Technology Letters*, 30(5), 2001, 327-330.
- [15]. Q. X. Niu, Y. J. Liu, D. J. Song, Y. J. Gao, C. L. Dai and H. W. Yang, Research of anti-ultraviolet nano-film structure based on the FDTD method, *Optik*, 127(2), 2016, 539-543.
- [16]. <http://www.optiwave.com/>.
- [17]. J. P. Berenger, A perfectly matched layer for the absorption of electromagnetic waves, *Journal of Computational Physics*, 114(2), 1994, 185-200.
- [18]. G. Makov, M. C. Payne, Periodic boundary conditions in ab initio calculations, *Physical Review B*, 51(7), 1995, 4014-4022.
- [19]. D. E. Palik, *Handbook of optical constant of solids*, (Academic press, 1998).
- [20]. M. J. Weber, *Handbook of lasers*, (CRC press, 2000).